

## Article

# U-Pb Age and Hf Isotope Systematics of Zircon from Eclogite Xenoliths in Devonian Kimberlites: Preliminary Data on the Archaean Roots in the Junction Zone between the Sarmatian and Fennoscandian Segments of the East European Platform

Leonid Shumlyansky <sup>1,\*</sup>, Stepan Tsybal <sup>2,†</sup>, Monika A. Kusiak <sup>3</sup>, Simon A. Wilde <sup>1</sup> , Alexander A. Nemchin <sup>1</sup>, Iryna Tarasko <sup>4</sup>, Liudmyla Shumlianska <sup>5</sup> and Mandy Hofmann <sup>6</sup>

<sup>1</sup> School of Earth and Planetary Sciences, Curtin University, GPO Box U1987, Perth, WA 6845, Australia; s.wilde@curtin.edu.au (S.A.W.); a.nemchin@curtin.edu.au (A.A.N.)

<sup>2</sup> M.P. Semenenko Institute of Geochemistry, Mineralogy and Ore Formation, Palladina Ave., 34, 03142 Kyiv, Ukraine; tsybal@igmof.gov.ua

<sup>3</sup> Institute of Geophysics, Polish Academy of Science, Ksiecia Janusza 64, PL-01452 Warsaw, Poland; monika.kusiak@igf.edu.pl

<sup>4</sup> Rivne Complex Geological Enterprise of the State Ukrainian Geological Company, Kurchatova 11, 33000 Rivne, Ukraine; sergevol@gmail.com

<sup>5</sup> S.I. Subbotin Institute of Geophysics of the NAS of Ukraine, Palladin Ave., 32, 03142 Kyiv, Ukraine; lashum@ukr.net

<sup>6</sup> Sektion Geochronologie, Senckenberg Naturhistorische Sammlungen Dresden (SNSD), Königsbrücker Landstraße 159, 01109 Dresden, Germany; mandy.hofmann@senckenberg.de

\* Correspondence: Leonid.Shumlyansky@curtin.edu.au

† Deceased.



**Citation:** Shumlyansky, L.; Tsybal, S.; Kusiak, M.A.; Wilde, S.A.; Nemchin, A.A.; Tarasko, I.; Shumlianska, L.; Hofmann, M. U-Pb Age and Hf Isotope Systematics of Zircon from Eclogite Xenoliths in Devonian Kimberlites: Preliminary Data on the Archaean Roots in the Junction Zone between the Sarmatian and Fennoscandian Segments of the East European Platform. *Geosciences* **2021**, *11*, 487. <https://doi.org/10.3390/geosciences11120487>

Academic Editors:

Jesus Martinez-Frias and Maurizio Barbieri

Received: 4 October 2021

Accepted: 22 November 2021

Published: 25 November 2021

**Publisher's Note:** MDPI stays neutral with regard to jurisdictional claims in published maps and institutional affiliations.



**Copyright:** © 2021 by the authors. Licensee MDPI, Basel, Switzerland. This article is an open access article distributed under the terms and conditions of the Creative Commons Attribution (CC BY) license (<https://creativecommons.org/licenses/by/4.0/>).

**Abstract:** The results of a laser ablation inductively coupled plasma mass spectrometry (LA-ICP-MS) U-Pb dating and a Hf isotope study of zircon crystals separated from small eclogite xenoliths found in Devonian kimberlites within the Prypyat horst, Ukraine, have been reported. The studied area is located in the junction zone between the Sarmatian and Fennoscandian segments of the East European Platform. Four laser ablation sites on two zircon grains yielded Paleoproterozoic U-Pb ages between  $1954 \pm 24$  and  $1735 \pm 54$  Ma. In contrast, three of four Hf sites revealed negative  $\epsilon_{\text{Hf}}$  values and Paleoproterozoic to Mesoarchean model ages, excluding the possibility that the eclogite xenoliths represented segments of a juvenile Paleoproterozoic subducted slab or younger mafic melts crystallized in the subcontinental lithospheric mantle. A single laser ablation Hf spot yielded a positive  $\epsilon_{\text{Hf}}$  value (+3) and a Paleoproterozoic model age. Two models for eclogite origin can be proposed. The first foresees the extension of the Archean lower-crustal or lithospheric roots beneath the Sarmatia–Fennoscandia junction zone for over 200 km from the nearest known outcrop of Archean rocks in the Ukrainian Shield. The second model is that the Central Belarus Suture Zone represents a rifted-out fragment of the Kola–Karelian craton that was accreted to Sarmatia before the actual collision of these two segments of Baltica.

**Keywords:** eclogite xenolith; kimberlite; zircon; U-Pb age; Hf isotopes; Ukrainian Shield; Devonian; East European Platform

## 1. Introduction

Eclogite is a metamorphic rock of basic (basaltic) composition predominantly made of garnet and Na-bearing clinopyroxene (omphacite) that is rare at the Earth surface. It indicates high-pressure (over 1.2 GPa) and relatively high-temperature (over 500 °C) conditions of metamorphic crystallization [1], which may be achieved either in the upper mantle or in the lowermost part of a thickened crust. Eclogites having MORB-like geochemistry are often considered as an evidence of subduction [2–7], and some have been used to suggest

the operation of global plate tectonics since the Paleoproterozoic [4,5,8–10]. In subduction zones, the eclogite mineral assemblage crystallizes due to the metamorphism of mafic rocks comprising the subducting plate. In contrast, a model in which eclogites represent primary igneous rocks that crystallize under high temperature and pressure conditions in the subcontinental lithospheric mantle was proposed by [11]. Finally, retrogressed eclogites from Paleoproterozoic orogens interpreted as mafic rocks metamorphosed at high pressure in a thickened crust were discussed by [5].

Eclogite xenoliths have been found in numerous kimberlite pipes worldwide [9,12–16]. The interpretation of their origins is not straightforward as the geological context is not always well understood, although these xenoliths are widely used to constrain lithosphere evolution, including the subduction of oceanic lithosphere.

In the Ukrainian Shield, mantle xenoliths occur in the Palaeoproterozoic and Devonian kimberlites [17–19], whereas eclogite xenoliths have been described only in kimberlite fragments found in the late Palaeozoic breccias within the Prypyat horst [18]. In this short communication, we reported results of U–Pb dating and Hf isotope studies of two rare zircon crystals that were extracted from small eclogite xenoliths. We discussed their possible meanings in understanding the geological history of the Ukrainian Shield in the Paleoproterozoic.

## 2. Geological Setting

### 2.1. The Prypyat Horst

The Prypyat horst is located in the northern part of the Volyn-Podillya Basin and represents a prolongation of the Prypyat branch of the middle to late Paleozoic Prypyat-Dnieper-Donets Paleorift (PDDP; Figure 1). The PDDP is located in the southwestern part of the East European platform and separates the Ukrainian Shield at the south from the Voronezh Crystalline massif in the north. A large volume of alkaline, ultramafic and mafic igneous rocks is known to be associated with the PDDP [20–31] and has been related to a mantle plume during the late Frasnian [25]. Kimberlites related to the PDDP are known in the Prypyat horst (see below) and in the junction between the Azov Domain of the Ukrainian Shield and the Donets Basin [26,32].

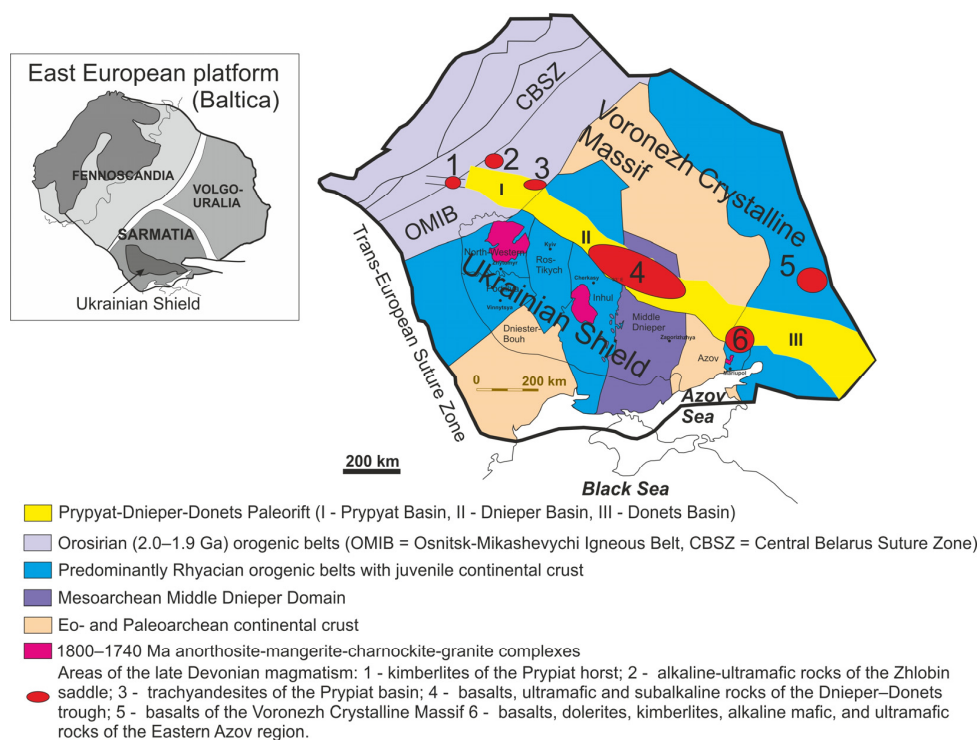


**Figure 1.** Schematic map of Sarmatia, modified after [32,33]. The positions of the Prypyat-Dnieper-Donets Paleorift and related magmatism are shown.

The Prypyat horst is a complex east-west trending structure limited by normal faults and disrupted by a series of transverse faults (Figure 2). It extends along the strike for 100–120 km and is 20–30 km in width. The crystalline basement in the western part of the horst is composed of Paleoproterozoic gneisses, amphibolites, gabbros and granitoids. This area has been interpreted as a part of the Central Belarusian Suture Zone, which represents a Paleoproterozoic belt extended along the Osnitsk-Mikashevychi Igneous Belt (OMIB) [34]. The Central Belarusian Suture Zone comprises amphibolite- to granulite-facies rocks units separated by the NE-trending Minsk Fault. The rock units occurring in the NW from the fault comprise ca. 2.0 Ga island-arc metavolcanic rocks (basalts and andesites), banded iron formation, black shales and calcareous metasediments [35]. All these rock types have been intruded by ca. 1.9 Ga plagioclase granitoids [36]. In contrast, rock units occurring in the SE of the Minsk Fault include predominantly metasediments, while ca. 1.98 Ga intermediate to felsic metavolcanic rocks are less spread [37].

The eastern part of the Prypyat horst belongs to the OMIB [38,39], which is considered to represent a Paleoproterozoic (ca. 2030–1980 Ma) active continental margin [40,41]. The OMIB comprises intrusive rocks ranging in composition from ultrabasics to granitoids (with granitoids being the predominant rock type) and extrusive rocks of basaltic and rhyolitic compositions metamorphosed under epidote-amphibolite facies conditions. Metasedimentary rocks are lacking in the OMIB. The nature and the exact position of the boundary between the Central Belarusian Suture Zone and the Osnitsk-Mikashevychi Igneous Belt are unknown.

The crystalline basement in the area is overlain by an 835 m-thick continental silt-sandy red-bed formation of the Polissya Series filling the Volyn-Orsha aulacogen. The maximum age of the Polissya Series is defined by the U–Pb dating of detrital zircons at ca. 1020 Ma [42,43].

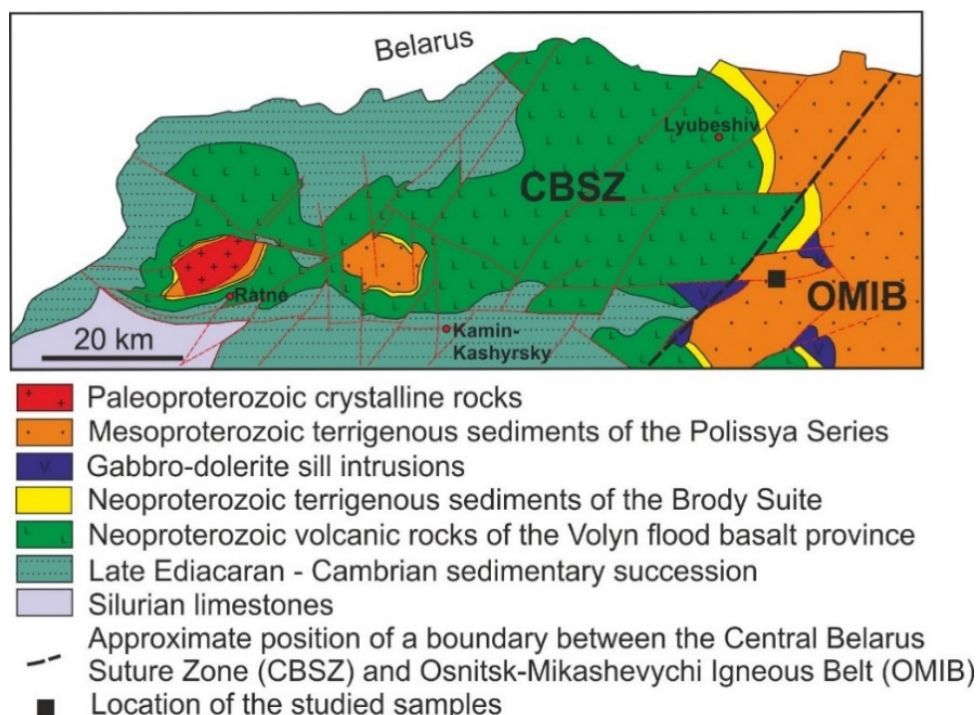


**Figure 2.** Schematic geological map and section across the Prypyat horst, simplified from [34].

The Polissya Series is overlain in places by terrigenous sediments of the Brody Suite that may exceed 20 m in thickness, which was almost entirely eroded already in Ediacaran Period. The Brody Suite comprises red-coloured sandstones that host small (up to 15 cm in size) granite boulders and quartz-feldspar pebbles. The upper part of the sequence gradually changes into siltstones that contain small fragments of crystalline rocks and

represents the stratigraphic equivalent of the much thicker (up to 483 m) Glusk Suite that belongs to the Ediacaran Vilcha Series in Belarus [44] and has been interpreted as representing glacial deposits [45].

The volcanogenic formations of the ca. 570 Ma Volyn Series overlie the sediments of the Polissya Series and Brody Suite. The thickness of the Volyn Series tuffs and basaltic flows reaches 300–500 m [46–48]. All these rocks were once overlain by Ediacaran to Silurian sediments that were mostly eroded within the Prypyat horst during its uplift in the Devonian.

## 2.2. Geophysical Data

According to [49], the Central Belarusian Suture Zone differs from the adjacent tectonic units (the OMIB in the SE and the Belarus-Baltic Granulite Belt in the NW) by generating higher seismic velocities in the crust and by the higher average rock densities, reaching 3.45 g/cm<sup>3</sup> below the Moho (in contrast to 3.30 g/cm<sup>3</sup> in the OMIB). The thickness of the crust varies from 50 to 55 km in both the Central Belarusian Suture Zone and the OMIB.

An southwest to south-southwest dipping reflector has been detected in the uppermost mantle by the EUROBRIDGE'97 seismic profile [50]. According to [49], this reflector may represent a relic of the subducted oceanic plate that corresponds to the closure of the ocean basin once located between Sarmatia and Fennoscandia. However, reference [50] noticed that the direction of the dip of the reflector is nearly perpendicular to the strike direction of the OMIB and the Central Belarus Suture Zone. Therefore, they suggested that the reflector may represent the trace of a suture between Sarmatia and Fennoscandia or a collision-related shear zone in the upper mantle.

The results of the quasi-three-dimensional (3D) seismotomographic P-wave modelling of the upper mantle beneath western Ukraine [51] at depths between 100 and 200 km are given in Figure 3. These data indicate that the Prypyat host is located at the edge of the high-velocity (and high-density) region that embraces Western Ukraine, including the western part of the Ukrainian Shield and its western slope. These high-density rocks revealed by seismic tomography indicate the possible presence of eclogites in the subcontinental lithospheric mantle.

## 2.3. Kimberlite Samples and Their Setting

The Prypyat horst is cut by the Kuhotska Volya and Belska zones of brecciated rocks that are interpreted as post-Silurian explosive structures confined to the fault zones [52]. These zones occur as pipe-like bodies having 75–250 m in size, filled with non-cemented fragments of various rocks, including sedimentary rocks, felsic to ultramafic tuffs, picrites, basalts, dolerites, lamprophyres and kimberlites. The youngest rock fragments found in these zones are limestone and dolomite of the late Silurian Ludlow group [53]. A few fragments of kimberlite and their indicator minerals (pyrope and picroilmenite) were recovered from breccias of the Kuhotska Volya zone [18,53]. Because of their economic potential, over 70 holes were drilled in the area, six of which have revealed over 60 kimberlite fragments. The size of these fragments varies from a few millimetres to 3–5 cm, rarely reaching 10 cm. The fragments are irregular in shape and have rough surfaces, without any evidence of mechanical abrasion. Kimberlites are represented by eruptive breccia that contains xenoliths of mantle rocks (see below) and minerals (olivine, Cr-spinel, Cr-diopside, pyrope and picroilmenite), fragments of earlier kimberlite, and fragments of the sedimentary rocks that constitute the platform cover in this area. All these are cemented by a kimberlite matrix of the basaltic (group I) type [18,54]. The most common size of xenoliths and fragments is 2–5 cm, and their amount may reach 30–50% of the total volume of the kimberlitic breccia, with fragments of sedimentary rocks being the most abundant. The kimberlitic cement is porphyritic and contains 20% to 70% of serpentine and serpentine-carbonate aggregates that are developed from primary olivine phenocrysts. The kimberlite groundmass is aphanitic to fine-grained, heavily altered, and composed of serpentine and carbonate. In places, it contains a large amount of opaque minerals.

Mantle xenoliths in the kimberlite breccia include eclogite, pyrope peridotite and ilmenite peridotite. Due to their small size (less than 1 cm), we were unable to obtain truly representative samples suitable for comprehensive geochemical and mineralogical studies. A few medium- to coarse-grained eclogite xenoliths were obtained, which contained completely replaced by secondary minerals omphacite and fresh garnet. One of the xenoliths contains altered olivine. Two largest xenoliths were processed individually in order to separate accessory minerals. These included apatite, rutile, ilmenite, and graphite.

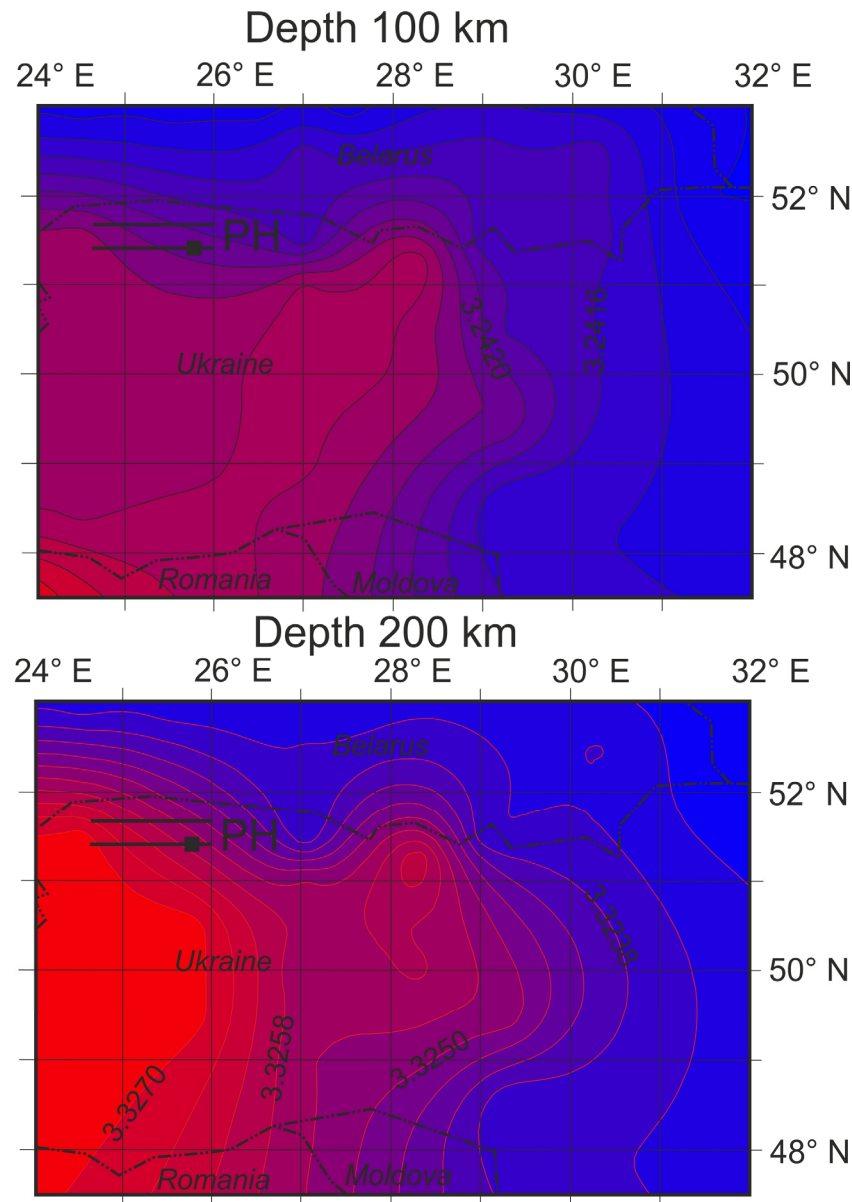


**Figure 3.** Horizontal seismotomographic sections of the mantle in Western Ukraine at depths from 100 and 200 km. The isolines indicate the calculated rock densities in  $\text{g}/\text{cm}^3$ . PH stands for the Prypyat horst, and the sampled area is shown by a black square.

#### 2.4. Zircon Description

Two zircon grains were isolated from two eclogite xenoliths. Grain 1 was euhedral, prismatic with poorly developed bipyramids,  $\sim 380 \mu\text{m}$  long, transparent, and light brownish-red in colour. Although it looks completely homogeneous under an optical microscope, the cathodoluminescence (CL) imaging revealed strong oscillatory zonation, with a dark irregular core and numerous light zones (Figure 4). Grain 2 was isometric,

anhedral, ~200 µm in size, transparent and grey-coloured. This grain was completely homogeneous both under an optical microscope and in CL (Figure 4).

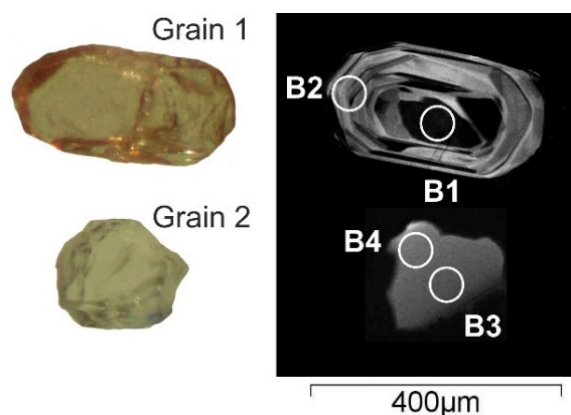


**Figure 4.** Optical microscopic and cathodoluminescence (CL) images of the two eclogite zircons.

### 3. Analytical Techniques

The samples were processed at the M.P. Semenenko Institute of Geochemistry, Mineralogy, and Ore Formation, Kyiv, Ukraine, employing conventional separation methods (a water shaking table, heavy liquids and a magnetic separator). Zircon grains were handpicked from a heavy mineral fraction under a binocular microscope LOMO MSP-1, mounted in a resin puck and polished to half of their thickness. The laser ablation inductively coupled plasma mass spectrometry (LA-ICP-MS) U–Pb dating of zircons was carried at the Geochronology section of the Senckenberg Natural History Collections in Dresden (SNSD) using a Thermo-Scientific Element 2 XR sector field ICP-MS, coupled to a New Wave UP-193 ArF Excimer Laser System. Each analysis consisted of 15 s background acquisition followed by 30 s data acquisition, using a laser spot-size of 35 µm. Raw data were corrected for background signals, laser-induced elemental fractionation, instrumental mass discrimination and time-dependant elemental fractionation of Pb/Th and Pb/U. The reported uncertainties were propagated by the quadratic addition of the external reproducibility obtained from the standard zircon GJ-1 (~0.6% and 0.5–1% for  $^{207}\text{Pb}/^{206}\text{Pb}$  and  $^{206}\text{Pb}/^{238}\text{U}$ , respectively). For further details on the analytical protocol and data processing, see [55]. Th/U ratios, together with U and Pb contents, were determined from the LA-ICP-MS data and calculated relative to the GJ-1 zircon standard; values were accurate to within approximately 10%.

The Lu–Hf analyses were performed using LA-ICP-MS at the Institute of Geology and Geophysics in the Chinese Academy of Sciences in Beijing. The Neptune instrument used was equipped with a 193 nm ArF excimer laser-ablation system. The analytical procedures are described in [56]. A laser repetition rate of 10 Hz at 100 mJ was used, and the spot size was 40 µm. To transport the ablated material from the laser-ablation cell to the ICMPS torch, He and Ar carrier gases were used. Raw count rates for  $^{172}\text{Yb}$ ,  $^{173}\text{Yb}$ ,  $^{175}\text{Lu}$ ,  $^{176}(\text{Hf}+\text{Yb}+\text{Lu})$ ,  $^{177}\text{Hf}$ ,  $^{178}\text{Hf}$ ,  $^{179}\text{Hf}$  and  $^{180}\text{Hf}$  were collected. The isobaric interference of  $^{176}\text{Lu}$  on  $^{176}\text{Hf}$  was corrected assuming  $^{176}\text{Lu}/^{175}\text{Lu} = 0.02655$  [57], and the mean mass bias value of Yb obtained during analysis on the same spot was applied for the interference correction of  $^{176}\text{Yb}$  on  $^{176}\text{Hf}$  [58], assuming a value of 0.5886 for  $^{176}\text{Yb}/^{172}\text{Yb}$ . During the analysis, the  $^{176}\text{Hf}/^{177}\text{Hf}$  and  $^{176}\text{Lu}/^{177}\text{Lu}$  ratios of the standard zircons, GJ-1 and Mud Tank [59] were  $0.2824988 \pm 0000035$  and  $0.2820155 \pm 0000040$ , respectively. The  $^{176}\text{Lu}$  decay constant used was  $1.867 \times 10^{-11} \text{ year}^{-1}$  [60].

## 4. Results

### 4.1. U–Pb Dating

Grain 1 yielded concordant ages of  $1954 \pm 24 \text{ Ma}$  (core part,  $^{207}\text{Pb}/^{206}\text{Pb}$  date) and  $1802 \pm 43 \text{ Ma}$  (outer part; Table 1; Figure 5). Two analyses carried out in grain 2 yielded

close to concordant (4% and 3% of discordance, respectively) results were shown as follows: the  $^{207}\text{Pb}/^{206}\text{Pb}$  date of  $1824 \pm 47$  Ma for the central part and that of  $1735 \pm 54$  Ma for the outer part.

**Table 1.** Results of the laser ablation inductively coupled plasma mass spectrometry (LA-ICP-MS) U–Pb dating of zircons from eclogite xenoliths.

Spot #	$^{207}\text{Pb}$		Isotope Ratios		$^{207}\text{Pb}$		Ages (Ma $\pm 2\sigma$ )		$^{207}\text{Pb}$	Degree of Concordance (%)	U Concentrations (ppm)	Th Concentrations (ppm)	Th/U Ratio	
	$^{235}\text{U}$	2 $\sigma$ (%)	$^{206}\text{Pb}$	2 $\sigma$ (%)	$^{206}\text{Pb}$	2 $\sigma$ (%)	$^{235}\text{U}$	$^{238}\text{U}$						
B1	5.9369	3.1	0.35933	2.8	0.90	0.1198	1.3	1967 $\pm$ 27	1979 $\pm$ 48	1954 $\pm$ 24	101	30	12	0.39
B2	4.9965	4.5	0.32898	3.8	0.85	0.1102	2.4	1819 $\pm$ 39	1833 $\pm$ 61	1802 $\pm$ 43	102	20	7	0.20
B3	4.7844	5.4	0.31114	4.8	0.88	0.1115	2.6	1782 $\pm$ 47	1746 $\pm$ 74	1824 $\pm$ 47	96	40	15	0.50
B4	4.3428	5.2	0.29660	4.3	0.82	0.1062	3.0	1702 $\pm$ 44	1674 $\pm$ 64	1735 $\pm$ 54	97	38	13	0.43

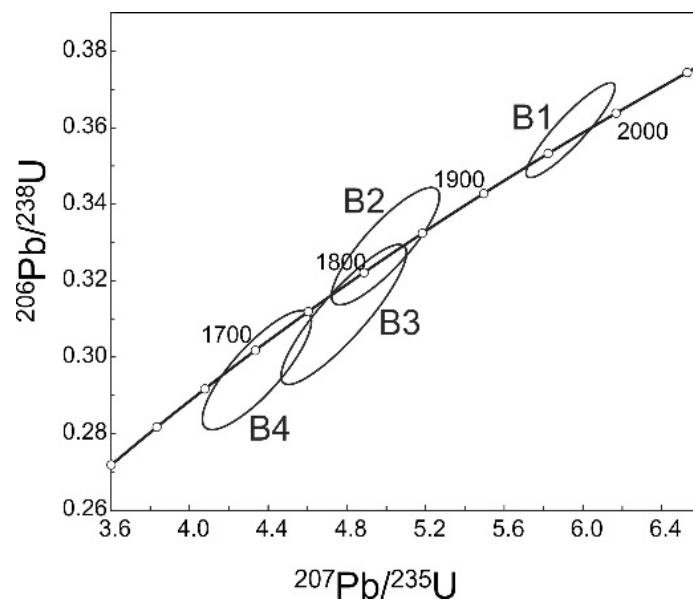


**Figure 5.** U–Pb concordia diagram for zircon analyses from the eclogite xenoliths.

4.2. Hf Isotopes

Hafnium isotope compositions were measured on the same spots as the U–Pb sites, and the results are reported in Table 2. Initial  $^{176}\text{Hf}/^{177}\text{Hf}$  and  $\epsilon\text{Hf}$  values were calculated according to  $^{207}\text{Pb}/^{206}\text{Pb}$  ages. All, except one, spots revealed low initial  $^{176}\text{Hf}/^{177}\text{Hf}$  ratios and negative  $\epsilon\text{Hf}$  values, and, correspondingly, Paleoproterozoic to Mesoproterozoic model ages. In contrast, a single spot (B4) located in the marginal part of the structureless grey zircon crystal yielded a positive  $\epsilon\text{Hf}$  value (+3) and a Paleoproterozoic model age.

**Table 2.** Hf isotope composition of zircons from eclogite xenoliths.

Spot #	$^{207}\text{Pb}/^{206}\text{Pb}$ Age (Ma)	Isotope Ratios				DM Model Ages (Ma)			
		$^{176}\text{Lu}/^{177}\text{Hf}$	$^{176}\text{Yb}/^{177}\text{Hf}$	$^{176}\text{Hf}/^{177}\text{Hf} \pm 1\sigma$	$^{176}\text{Hf}/^{177}\text{Hf}_T$	$\epsilon\text{Hf}_T \pm 2\sigma$	Actual Lu/Hf	Felsic Crust	Mafic Crust
Grain 1									
B1	1954	0.000087	0.002696	0.281211 $\pm$ 17	0.281207	−12 $\pm$ 1	2778	3103	3929
B2	1802	0.000031	0.000915	0.281168 $\pm$ 15	0.281166	−17 $\pm$ 1	2831	3234	4259
Grain 2									
B3	1824	0.000687	0.018131	0.281738 $\pm$ 14	0.281714	3 $\pm$ 1	2106	2211	2492
B4	1735	0.001255	0.035319	0.281156 $\pm$ 16	0.281114	−20 $\pm$ 1	2938	3354	4508

Note: Depleted mantle (DM) model ages were calculated using the measured  $^{176}\text{Lu}/^{177}\text{Hf}$  ratios, whereas “felsic crust” model ages were calculated using the average continental crust  $^{176}\text{Lu}/^{177}\text{Hf}$  of 0.015 [61] and “mafic crust” model ages were calculated using the  $^{176}\text{Lu}/^{177}\text{Hf}$  ratio of 0.021 [62].

## 5. Discussion

### 5.1. Origins of Zircons and Their Ages

The studied zircon crystals were separated from two small eclogite xenoliths. Hence, zircons in this rock could be igneous, metamorphic or xenogenic [63]. The Th/U ratios of the analysed sites varied from 0.20 to 0.50. Crystal 1 preserved the morphology and internal structure typical of igneous zircon, whereas grain 2 resembled those found in high-grade metamorphic rocks of the Ukrainian Shield [64]. Despite the lack of internal structure of grain 2, it revealed significant variations in Hf isotope composition (Table 2).

The zircon crystals yielded Paleoproterozoic ages in the range of 1955 to 1735 Ma ( $^{207}\text{Pb}/^{206}\text{Pb}$  ages). The three younger ages (1825–1735 Ma) were broadly coeval with the time assumed for the oblique collision of the Volgo-Sarmatian and Fennoscandian segments of the East European craton that started at ca. 1.83–1.81 Ga [65–67] (and continued for the next ~100 Myr, causing the rotation of Sarmatia [68]). At the same time, the Prutivka-Novogol large igneous province formed, consisting of numerous mantle-derived mafic and ultramafic dykes and large anorthosite–mangerite–charnockite–granite complexes [69–71].

In contrast, the single older age ( $1954 \pm 24$ ) corresponds to the formation of the Central Belarus Suture Zone [49] (and the first author's unpublished data). In general, the location of the results along the concordia line in the U–Pb isotope diagram (Figure 5) suggested that the younger ages may represent the result of resetting of the U–Pb isotope system. The locations of the three results close to the Pb-loss line in the  $\epsilon\text{Hf}$  vs. age plot (Figure 6) supported such a suggestion. In contrast, one of the spots yielded an elevated  $^{176}\text{Hf}/^{177}\text{Hf}$  ratio and correspondingly a high  $\epsilon\text{Hf}$  value (+3) at 1824 Ma, indicating the input of juvenile materials at that time. This Hf isotope composition was similar to that of zircons from the ca. 1780 Ma mafic dykes in the North-Western region of the Ukrainian Shield [72].

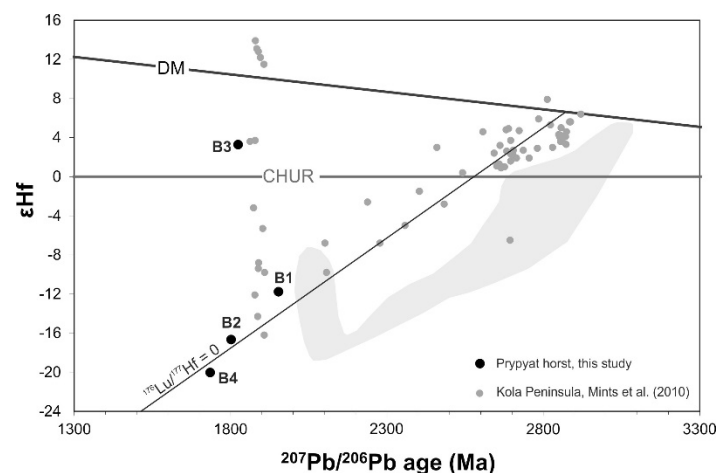


**Figure 6.** Diagram showing variations of  $\epsilon\text{Hf}$  values in zircons vs. age. Zircons from eclogites in the Kola Peninsula and granulites of the western part of the Ukrainian Shield (shown as a shaded field; [64,73,74]) were plotted for the comparison with the data from the present study.

The three analyses that were plotted close to the Pb-loss line yielded Meso- to Paleoproterozoic Hf model ages (Table 2), indicating an Archean protolith age for the eclogite xenoliths. This excluded the possibility that the eclogite xenoliths represented either the Paleoproterozoic subducted slab or mafic melts crystallized in the subcontinental lithospheric mantle. Grain 1, which had a preserved bipyramidal-prismatic shape and a concentric zoning, may represent a primary igneous zircon. The central part of grain 2 records a significant input of juvenile Paleoproterozoic materials, which can be related to the emplacement of the Prutivka-Novogol large igneous province [69,72]. In contrast, the younger outer part had an Archean Hf isotope signature, suggesting that the older, unradiogenic Hf derived during the recrystallization of the Archean protolith prevailed at the later stages of zircon

crystallization. These data indicated a complex geological history of the eclogite xenoliths. Our interpretation must be treated with caution, as it is based on a very limited dataset.

### 5.2. The Possible Protolith of the Eclogites

The Archean Hf isotope signature of eclogitic zircons from the Prypyat horst raises the question about the nature of the possible protolith. Both the OMIB and the Teteriv Belt represent juvenile Paleoproterozoic crust formed outboard of the Archean Dniester-Bouh Domain of the Ukrainian Shield, whereas Archean rock complexes are absent in the area. No Archean signature has been revealed in either the OMIB [41] or the Teteriv Belt [75,76]. The lower-crustal xenoliths of feldspar-rich garnet granulites and feldspar-poor eclogitic granulites that geochemically resemble mafic rocks of the OMIB have been also studied [77]. These xenoliths yielded Paleoproterozoic Nd model ages, despite the moderate contamination by the Devonian alkaline magmas that delivered them to the surface.

The nearest rocks, with the evidence of an Archaean protolith, to the Prypyat horst occurs at a distance of ca. 200 km, near the junction point of the North-Western, Podillya and Ros-Tikych regions of the Ukrainian Shield [78]. In terms of Nd and Hf isotopes, these rocks are indistinguishable from Mesoarchean rocks of the Dniester-Bouh Domain, which shows juvenile compositions at ca. 2800–3000 Ma. This rock assemblage has experienced a second metamorphic and igneous event (coeval with the formation of the Teteriv belt) at ca. 2100 Ma, which was accompanied by some input of juvenile materials. Zircons having ages between these two events plot on the Pb-loss line are shown in the grey field in Figure 6.

However, the Hf isotope systematics of zircons from eclogite xenoliths in the Devonian kimberlites did not match those in zircons from the Dniester-Bouh Domain. Instead, they had elevated  $^{176}\text{Hf}/^{177}\text{Hf}$  ratios. Theoretically, their isotope composition can be explained by a mixing of the prevailing old hafnium having a low  $^{176}\text{Hf}/^{177}\text{Hf}$  ratio with some amount of young juvenile Hf having an elevated  $^{176}\text{Hf}/^{177}\text{Hf}$  ratio.

Zircons from eclogite xenoliths of the Prypyat horst had isotope compositions similar to those found in zircons from retrograded eclogites of the Kola Peninsula [79] (Figure 6). They were all plotted on the same (or near the) Pb-loss line that intersects the depleted mantle curve at ca. 2.8 Ga. A single spot (B3) with a positive  $\epsilon\text{Hf}$  value found in the Prypyat zircon was also plotted close to the field of ca. 1900 Ma juvenile zircons recorded in the Kola Peninsula eclogites.

Looking at the broader regional correlation, a possible affiliation of the Central Belarus Suture Zone to Fennoscandia has been discussed by [49]. These authors suggested that the zone formed at the SE margin of the Fennoscandian plate and was attached to the OMIB during the collision of Sarmatia and Fennoscandia. However, this model does not fit the younger ages of the continental crust located in the northwest of the Central Belarus Suture Zone [33]. Geochronological data indicated that the vast areas of the continental crust between the Central Belarus Suture Zone and the Kola-Karelian craton (the core of Fennoscandia) did not yet exist at the time when the Central Belarus Suture Zone formed. The belonging of the Central Belarus Suture Zone to Sarmatia has been supported by the results of geological [80] and geophysical [81] studies.

If we accept the Meso- to Neoproterozoic age of the protolith of eclogite xenoliths, as revealed by the Hf isotope systematics of the rare zircon grains, then two possible explanations can be proposed for the origin of the eclogite. The first model involves the extension of the Archean lower-crust or lithospheric roots of the Dniester-Bouh Domain beneath the Teteriv and Osnitsk-Mikashevychi Belts and the Central Belarus Suture Zone for over 200 km from the nearest known outcrop of Archean rocks in the Ukrainian Shield. However, this model contradicts the well-known juvenile Paleoproterozoic nature of the Teteriv and Osnitsk-Mikashevychi belts. Moreover, the Hf isotope systematics of the eclogitic zircons does not match those in the Archean rocks of the Dniester-Bouh Domain. The second model indicates that the Central Belarus Suture Zone may represent a rifted fragment of the Kola-Karelian craton that was accreted to Sarmatia before the actual collision of these two segments of Baltica. The Central Belarus Suture Zone differs from the surrounding

areas by the denser crust, as recorded by the geophysical data, and the higher degree of metamorphism, reaching granulite facies. This is in marked contrast to the weakly metamorphosed surrounding areas. However, the substantiation of this model requires further detailed studies of the Central Belarus Suture Zone.

## 6. Conclusions

Zircons from two eclogite xenoliths in Devonian kimberlites had U–Pb ages in the range of 1955 to 1735 Ma ( $^{207}\text{Pb}/^{206}\text{Pb}$  ages), which corresponded to the ages of the rock assemblage constituting the Central Belarusian Suture Zone. However, Hf isotopes indicated Paleoproterozoic to Mesoproterozoic model ages for zircon crystals in eclogite xenoliths. Moreover, the Hf isotope systematics of the studied zircons revealed the affinity of the protolith to the Fennoscandian segment of Baltica rather than to Sarmatia.

The nature of the eclogite protolith remains unresolved, as it may represent either a fragment of the subducted Archean lithosphere or Archean mafic rocks that crystallized from the plume-related mafic melts in the thickened lower crust or upper mantle. Geophysical data support the presence of mantle rocks having the increased density in the area. At ca. 1800 Ma, the eclogite protolith experienced some rejuvenation probably due to the emplacement of mafic melts related to the Prutivka-Novogol large igneous province. Irrespective of the exact origin, the newly obtained results presented here indicated a complex geological history for the junction zone between the Sarmatian and Fennoscandian segments of the East European Platform (Baltica). A further detailed geochronological and isotope geochemical study of the rock complexes composing the junction zone is required.

**Author Contributions:** Conceptualization, L.S. (Leonid Shumlyansky) and S.T.; formal analysis, M.A.K., I.T., L.S. (Liudmyla Shumlianska) and M.H.; investigation, L.S. (Leonid Shumlyansky) and S.T.; writing—original draft preparation, L.S. (Leonid Shumlyansky); writing—review and editing, M.A.K., S.A.W., A.A.N. and M.H.; supervision, A.A.N. All authors have read and agreed to the published version of the manuscript.

**Funding:** This research received no external funding.

**Institutional Review Board Statement:** Not applicable.

**Informed Consent Statement:** Not applicable.

**Data Availability Statement:** All the analytical data are presented in the paper.

**Acknowledgments:** We acknowledge the Curtin Research Office for providing support to L.S. The paper has benefitted from constructive comments from two anonymous reviewers.

**Conflicts of Interest:** The authors declare no conflict of interest.

## References

1. Hacker, B.R. Eclogite formation and the rheology, buoyancy, seismicity, and H<sub>2</sub>O content of oceanic crust. In *Subduction Top to Bottom*; Bebout, G.E., Scholl, D.W., Kirby, S.H., Platt, J.P., Eds.; AGU: Washington, DC, USA, 1996. [\[CrossRef\]](#)
2. Becker, H.; Jochum, K.P.; Carlson, R.W. Trace element fractionation during dehydration of eclogites from high-pressure terranes and the implications for element fluxes in subduction zones. *Chem. Geol.* **2000**, *163*, 65–99. [\[CrossRef\]](#)
3. Boniface, N.; Schenk, V.; Appel, P. Paleoproterozoic eclogites of MORB-type chemistry and three Proterozoic orogenic cycles in the Ubendian Belt (Tanzania): Evidence from monazite and zircon geochronology, and geochemistry. *Precam. Res.* **2012**, *192–195*, 16–33. [\[CrossRef\]](#)
4. François, C.; Debaille, V.; Paquette, J.-L.; Baudet, D.; Javaux, E.J. The earliest evidence for modern-style plate tectonics recorded by HP–LT metamorphism in the Paleoproterozoic of the Democratic Republic of the Congo. *Sci. Rep.* **2018**, *8*, 15452. [\[CrossRef\]](#)
5. Loose, D.; Schenk, V. 2.09 Ga old eclogites in the Eburnian-Transamazonian orogen of southern Cameroon: Significance for Palaeoproterozoic plate tectonics. *Precam. Res.* **2018**, *304*, 1–11. [\[CrossRef\]](#)
6. Möller, A.; Appel, P.; Mezger, K.; Schenk, V. Evidence for a 2 Ga subduction zone: Eclogites in the Usagaran belt of Tanzania. *Geology* **1995**, *23*, 1067–1070. [\[CrossRef\]](#)
7. Palin, R.M.; Dyck, B. Metamorphic consequences of secular changes in oceanic crust composition and implications for uniformitarianism in the geological record. *Geosci. Front.* **2018**, *9*, 1009–1019. [\[CrossRef\]](#)
8. Palin, R.M.; Santosh, M. Plate tectonics: What, where, why, and when? *Gondwana Res.* **2020**, *100*, 3–24. [\[CrossRef\]](#)

9. Shchukina, E.V.; Agashev, A.M.; Golovin, N.N.; Pokhilenko, N.P. Equigranular Eclogites from the V. Grib Kimberlite Pipe: Evidence for Paleoproterozoic Subduction on the Territory of the Arkhangelsk Diamondiferous Province. *Dokl. Earth Sci.* **2015**, *462*, 497–501. [[CrossRef](#)]
10. Shchukina, E.V.; Agashev, A.M.; Zedgenizov, D.A. Origin of zircon-bearing mantle eclogites entrained in the V. Grib kimberlite (Arkhangelsk region, NW Russia): Evidence from mineral geochemistry and the U-Pb and Lu-Hf isotope compositions of zircon. *Mineral. Petrol.* **2018**, *112*, 85–100. [[CrossRef](#)]
11. Griffin, W.L.; O'Reilly, S.Y. Cratonic lithospheric mantle: Is anything subducted? *Episodes* **2007**, *30*, 43–53. [[CrossRef](#)] [[PubMed](#)]
12. Agashev, A.M.; Pokhilenko, L.N.; Pokhilenko, N.P.; Shchukina, E.V. Geochemistry of eclogite xenoliths from the Udachnaya Kimberlite Pipe: Section of ancient oceanic crust sampled. *Lithos* **2018**, *314–315*, 187–200. [[CrossRef](#)]
13. Barth, M.G.; Rudnick, R.L.; Horn, I.; McDonough, W.F.; Spicuzza, M.J.; Valley, J.W.; Haggerty, S.E. Geochemistry of xenolithic eclogites from West Africa, Part I: A link between low MgO eclogites and Archean crust formation. *Geochim. Cosmochim. Acta* **2001**, *65*, 1499–1527. [[CrossRef](#)]
14. Barth, M.G.; Rudnick, R.L.; Horn, I.; McDonough, W.F.; Spicuzza, M.J.; Valley, J.W.; Haggerty, S.E. Geochemistry of xenolithic eclogites from West Africa, part 2: Origins of the high MgO eclogites. *Geochim. Cosmochim. Acta* **2002**, *66*, 4325–4345. [[CrossRef](#)]
15. Heaman, L.M.; Creaser, R.A.; Cookenboo, H.O.; Chacko, T. Multi-Stage Modification of the Northern Slave Mantle Lithosphere: Evidence from Zircon- and Diamond-Bearing Eclogite Xenoliths Entrained in Jericho Kimberlite, Canada. *J. Petrol.* **2006**, *47*, 821–858. [[CrossRef](#)]
16. Sun, J.; Rudnick, R.L.; Kostrovitsky, S.; Kalashnikova, T.; Kitajima, K.; Li, R.; Shu, Q. The origin of low-MgO eclogite xenoliths from Obnazhennaya kimberlite, Siberian craton. *Contrib. Mineral. Petrol.* **2020**, *175*, 25. [[CrossRef](#)]
17. Shumlyanskyy, L.; Mitrokhin, O.; Billström, K.; Ernst, R.; Vishnevskaya, E.; Tsymbal, S.; Cuney, M.; Soesoo, A. The ca. 1.8 Ga mantle plume related magmatism of the central part of the Ukrainian shield. *GFF* **2016**, *138*, 86–101. [[CrossRef](#)]
18. Tsymbal, S.N. Kimberlites of the central part of the Prypyat swell, Ukraine. *Mineral. J. (Ukr.)* **2003**, *25*, 70–87. (In Russian)
19. Tsymbal, S.N.; Kryvdik, S.G. Xenoliths of deep-seated rocks from kimberlites of the Kirovograd area, Ukrainian shield. *Mineral. J. (Ukr.)* **1999**, *21*, 97–111. (In Russian)
20. Korzun, V.P.; Makhnach, A.S. *Upper Devonian Alkaline Association of the Prypyat Basin*; Nauka i Tekhnika: Minsk, Belarus, 1977; 154p. (In Russian)
21. Pervov, V.A.; Nikitin, E.A.; Levskiy, L.K. Ultramafic alkaline volcanic rocks of the Zlobino field (Republic of Belarus): Sources and evolution of the magmas. *Petrology* **2004**, *12*, 354–373. (In Russian)
22. Mikhailov, N.D.; Laptsevich, A.G.; Vladykin, N.V. Sr and Nd isotope composition in the Devonian alkaline igneous rocks. *Litasfera* **2011**, *35*, 113–122. (In Russian)
23. Aizberg, Y. Pripyat area of the Late-Devonian magmatism and its association with the plume tectonics of the Dnieper lithosphere segment. *Dokl. Natl. Acad. Sci. Belarus* **2019**, *63*, 597–607. (In Russian) [[CrossRef](#)]
24. Kuzmenkova, O.F.; Laptsevich, A.G.; Nosova, A.A. The Upper Devonian magmatic complexes of the south-east Belarus. *Dokl. Natl. Acad. Sci. Belarus* **2020**, *64*, 599–608. (In Russian) [[CrossRef](#)]
25. Wilson, M.; Lyashkevich, Z.M. Magmatism and the geodynamics of rifting of the Pripyat-Dnieper-Donets rift, East European platform. *Tectonophysics* **1996**, *268*, 65–81. [[CrossRef](#)]
26. Yutkina, E.V.; Kononova, V.A.; Bogatkov, O.A.; Knyazkov, A.P.; Kozar, N.A.; Ovchinnikova, G.V.; Levskiy, L.K. Kimberlites of the eastern Priazove (Ukraine) and geochemical characteristics of their sources. *Petrology* **2004**, *12*, 134–148.
27. Yutkina, E.V.; Nosova, A.A.; Sazonova, L.V.; Larionova, Y.O.; Kondrashov, I.A.; Shumlyanskyy, L.V.; Albekov, A.Y.; Savko, K.A. Devonian volcanics in the Voronezh crystalline Massif, East European Platform: Evolution of the melts and characteristics of crustal contamination. *Petrology* **2017**, *25*, 241–271. [[CrossRef](#)]
28. Sazonova, L.V.; Nosova, A.A.; Yutkina, E.V.; Kondrashov, I.A.; Shumlyanskyy, L.V. Genesis and evolution of mantle melts of the Devonian mafic-ultramafic rocks from the Eastern Azov region (Dnieper-Donets rift, Ukraine): Evidence from clinopyroxene geochemistry. *Petrology* **2019**, *27*, 633–654. [[CrossRef](#)]
29. Buturlinov, N.V. Magmatism in the Graben-Like Basins of the Southern East European Platform in Phanerozoic. Ph.D. Thesis, Donetsk Polytechnic Institute, Donetsk, Ukraine, 1979; 484p. (In Russian)
30. de Boorder, H.; van Beek, A.J.J.; Dijkstra, A.H.; Galetsky, L.S.; Koldewe, G.; Panov, B.S. Crustal architecture of the Donets Basin: Tectonic implications for diamond and mercury-antimony mineralization. *Tectonophysics* **1996**, *268*, 293–309. [[CrossRef](#)]
31. Sheremet, E.M.; Kryvdik, S.G.; Kozar, N.A.; Strekozov, S.N.; Vovkotrub, N.V.; Setaya, L.D.; Nikolayev, I.Y.; Agarkova, N.G.; Dubina, A.V.; Gatsenko, V.A.; et al. *Phanerozoic Magmatism of the Eastern Azov Area of the Ukrainian Shield and Related Commercial Minerals (Petrology, Geochemistry, and Ore Potential)*; Comprint Publisher: Kyiv, Ukraine, 2015; 318p. (In Russian)
32. Shumlyanskyy, L.V.; Kamenetsky, V.S.; Tsymbal, S.M.; Wilde, S.A.; Nemchin, A.A.; Ernst, R.E.; Shumlyanskaya, L.O. Zircon megacrysts from Devonian kimberlites of the Azov Domain, Eastern part of the Ukrainian Shield: Implications for the origin and evolution of kimberlite melts. *Lithos* **2021**, *406–407*, 106528. [[CrossRef](#)]
33. Bogdanova, S.V.; Gorbatshev, R.; Garetzky, R.G. *Europe/East European Craton Reference Module in Earth Systems and Environmental Sciences*; Elsevier: Amsterdam, The Netherlands, 2016; pp. 1–18.
34. Melnychuk, G.V. The Paleoproterozoic crystalline basement of the Volyn Paleozoic uplift: Peculiarities of the construction and geological history. *Geol. Zhurnal* **2013**, *4*, 24–32. (In Ukrainian)

35. Kozlovskaya, E.; Taran, L.; Karatayev, G.; Astapenko, V.; Yliniemi, J. Structure of the lithosphere along the CEL05 profile in Belarus (western part of the East European Craton): Constraints from geological and non-seismic geophysical data. *Litasfera* **2013**, *38*, 75–92.
36. Shcherbak, N.P.; Pap, A.M.; Bartnitsky, E.N.; Zayats, A.P. The uranium-lead isotopic age of granitoids in Belorussia. In *Doklady Akademii Nauk Belarusi*; Akademii Nauk Belarusi: Minsk, Belarus, 1990; Volume 34, pp. 740–743. (In Russian)
37. Bogdanova, S.V.; Bibikova, E.V.; Gorbachev, R. Palaeoproterozoic U-Pb zircon ages from Belorussia: New tectonic implications for the East European Craton. *Precambr. Res.* **1994**, *68*, 231–240. [[CrossRef](#)]
38. Aksamentova, N.V.; Tolkachikova, A.A. *Petrography and Geochemistry of the Crystalline Basement of Belarus*; BelNIGRI: Minsk, Belarus, 2012; pp. 1–232. (In Russian)
39. Krzeminska, E.; Krzeminski, L.; Wiszniewska, J.B.; Demaiffe, D.; Johansson, Å.E.; Williams, I.S. *Geological Map of Crystalline Basement in the Polish Part of the East European Platform 1:1,000,000*; Polish Geological Institute: Warsaw, Poland, 2017.
40. Claesson, S.; Bogdanova, S.V.; Bibikova, E.V.; Gorbatshev, R. Isotopic evidence for Palaeoproterozoic accretion in the basement of the East European Craton. *Tectonophysics* **2001**, *339*, 1–18. [[CrossRef](#)]
41. Shumlyansky, L.V. Geochemistry of the Osnitsk–Mikashevichy volcanoplutonic complex of the Ukrainian Shield. *Geochem. Int.* **2014**, *52*, 912–924. [[CrossRef](#)]
42. Shumlyansky, L.; Hawkesworth, C.; Dhuime, B.; Billström, K.; Claesson, S.; Storey, C.  $^{207}\text{Pb}/^{206}\text{Pb}$  ages and Hf isotope composition of zircons from sedimentary rocks of the Ukrainian shield: Crustal growth of the south-western part of East European craton from Archaean to Neoproterozoic. *Precam. Res.* **2015**, *260*, 39–54. [[CrossRef](#)]
43. Paszkowski, M.; Budzyń, B.; Mazur, S.; Sláma, J.; Shumlyansky, L.; Środoń, J.; Dhuime, B.; Kędzior, A.; Liivamägi, S.; Pisarzowska, A. Detrital zircons U-Pb and Hf constraints on provenance and timing of deposition of the Mesoproterozoic to Cambrian sedimentary cover of the East European Craton, Belarus. *Precam. Res.* **2019**, *331*, 105352. [[CrossRef](#)]
44. Makhnach, A.S.; Garetsky, R.G.; Matveev, A.V. *Geology of Belarus*; Institute of Geological Sciences: Minsk, Belarus, 2001; 815p. (In Russian)
45. Chumakov, N.M. Precambrian tillites and tillitoids (the problem of the Precambrian glaciations). *Works GIN* **1978**, *308*, 1–204. (In Russian)
46. Kuzmenkova, O.F.; Nosova, A.A.; Shumlyansky, L.V. A comparison of the Neoproterozoic Volyn-Brest magmatic province with large continental flood basalt provinces of the world, the nature of low-Ti and high-Ti basic magmatism. *Litasfera* **2010**, *33*, 3–16. (In Russian)
47. Shumlyansky, L.; Nosova, A.; Billström, K.; Söderlund, U.; Andréasson, P.-G.; Kuzmenkova, O. The U-Pb zircon and baddeleyite ages of the Neoproterozoic Volyn Large Igneous Province: Implication for the age of the magmatism and the nature of a crustal contaminant. *GFF* **2016**, *138*, 17–30. [[CrossRef](#)]
48. Shumlyansky, L.V.; Andréasson, P.G.; Buchan, K.L.; Ernst, R.E. The Volynian Flood Basalt Province and coeval (Ediacaran) magmatism in Baltoscandia and Laurentia. *Mineral. J. (Ukr.)* **2007**, *29*, 47–55.
49. Garetsky, R.G.; Karatayev, G.I. A tectonogeodynamic model for the junction zone between the Fennoscandian and Sarmatian segments of the East European Platform. *Russ. Geol. Geophys.* **2011**, *52*, 1228–1235. [[CrossRef](#)]
50. Thibo, H.; Janik, T.; Omelchenko, V.D.; Grad, M.; Garetsky, R.G.; Belinsky, A.A.; Karatayev, G.I.; Zlotski, G.; Knudsen, M.E.; Sand, R.; et al. Upper lithosphere seismic velocity structure across the Pripyat Trough and Ukrainian Shield along the EU-RUBRIDGE' 97 profile. *Tectonophysics* **2003**, *371*, 41–79. [[CrossRef](#)]
51. Shumlianska, L.O.; Tripolsky, A.A.; Tsvetkova, T.A. The influence of the crust velocity structure on the results of seismic tomography of the Ukrainian Shield. *Geophys. J.* **2014**, *36*, 95–117. (In Russian)
52. Heiko, Y.V.; Tarasko, I.V.; Prykhodko, V.L.; Drozdetskyi, V.V.; Shymkiv, L.M. Perspectives of detection of deposits of diamonds in the Kohotsko-Bilska area. *Mineral. Resour. Ukr.* **2018**, *2*, 10–20. (In Ukrainian)
53. Volovnik, B.Y.; Vlasov, B.I.; Zlobenko, I.F.; Lavrov, D.A. On the composition and age of breccia of the central part of the Prypyat swell. *Geochem. Ore Form.* **1980**, *8*, 19–28. (In Russian)
54. Tsybal, S.N.; Kryvdik, S.G. On the composition of kimberlites of Ukraine. In *The Current State, Prospective and Directions for Further Exploration for Diamonds in Ukraine*; UkrDGRI: Kyiv, Ukraine, 2004; pp. 136–143. (In Russian)
55. Gerdes, A.; Zeh, A. Combined U-Pb and Hf isotope LA-(MC-) ICP-MS analysis of detrital zircons: Comparison with SHRIMP and new constraints for the provenance and age of an Armorican metasediment in Central Germany. *Earth Planet. Sci. Lett.* **2006**, *249*, 47–61. [[CrossRef](#)]
56. Wu, F.Y.; Yang, Y.H.; Xie, L.W.; Yang, J.H.; Xu, P. Hf isotopic compositions of the standard zircons and baddeleyites used in U-Pb geochronology. *Chem. Geol.* **2006**, *234*, 105–126. [[CrossRef](#)]
57. Machado, N.; Simonetti, A. U-Pb dating and Hf isotopic composition of zircon by laser-ablation MC-ICPMS. In *Laser Ablation-ICPMS in the Earth Sciences: Principles and Applications*; Sylvester, P., Ed.; Mineral. Assoc.: St. John's, NL, Canada, 2001; pp. 121–146.
58. Iizuka, T.; Hirata, T. Improvements of precision and accuracy in in-situ Hf isotope microanalysis of zircon using the laser ablation-MC-ICPMS technique. *Chem. Geol.* **2005**, *220*, 121–137. [[CrossRef](#)]
59. Morel, M.L.A.; Nebel, O.; Nebel-Jacobsen, Y.J.; Miller, J.S.; Vroon, P.Z. Hafnium isotope characterization of the GJ-1 zircon and reference material by solution and laser-ablation MC-ICPMS. *Chem. Geol.* **2008**, *255*, 231–235. [[CrossRef](#)]

60. Söderlund, U.; Patchett, P.J.; Vervoort, J.D.; Isachsen, C.E. The  $^{176}\text{Lu}$  decay constant determined by Lu-Hf and U-Pb isotope systematics of Precambrian mafic intrusions. *Earth Planet. Sci. Lett.* **2004**, *219*, 311–324. [[CrossRef](#)]
61. Griffin, W.L.; Belousova, E.A.; Shee, S.R.; Pearson, N.J.; O'Reilly, S.Y. Archean crustal evolution in the northern Yilgarn Craton: U–Pb and Hf-isotope evidence from detrital zircons. *Precam. Res.* **2004**, *131*, 231–282. [[CrossRef](#)]
62. Kemp, A.I.S.; Hawkesworth, C.J.; Paterson, B.A.; Kinny, P.D. Episodic growth of the Gondwana supercontinent from hafnium and oxygen isotopes in zircon. *Nature* **2006**, *439*, 580–583. [[CrossRef](#)]
63. Melnik, A.E.; Korolev, N.M.; Skublov, S.G.; Müller, D.; Li, Q.-L.; Li, X.-H. Zircon in mantle eclogite xenoliths: A review. *Geol. Mag.* **2021**, *158*, 1371–1382. [[CrossRef](#)]
64. Shumlyanskyy, L.; Wilde, S.A.; Nemchin, A.A.; Claesson, S.; Billström, K.; Bagiński, B. Eoarchean rock association in the Dniester-Bouh Domain of the Ukrainian shield: A suite of LILE-depleted enderbites and mafic granulites. *Precam. Res.* **2021**, *352*, 106001. [[CrossRef](#)]
65. Bogdanova, S.; Gorbatshev, R.; Grad, M.; Janik, T.; Guterch, A.; Kozlovskaya, E.; Motuza, G.; Skridlaite, G.; Starostenko, V.; Taran, L.; et al. EUROBRIDGE: New insight into the geodynamic evolution of the East European Craton. In *European Lithosphere Dynamics*; Gee, D.G., Stephenson, R.A., Eds.; The Geological Society of London: London, UK, 2006; Volume 32, pp. 599–625. [[CrossRef](#)]
66. Elming, S.-Å.; Shumlyanskyy, L.; Kravchenko, S.; Layer, P.; Söderlund, U. Proterozoic Basic dykes in the Ukrainian Shield: A palaeomagnetic, geochronologic and geochemical study—The accretion of the Ukrainian Shield to Fennoscandia. *Precam. Res.* **2010**, *178*, 119–135. [[CrossRef](#)]
67. Lubnina, N.V.; Bogdanova, S.V.; Shumlyanskyy, L.V. East-European craton in the Paleoproterozoic: New palaeomagnetic determinations on igneous complexes of the Ukrainian Shield. *Geofizika (Geophys.)* **2009**, *5*, 56–64. (In Russian)
68. Bogdanova, S.V.; Gintov, O.B.; Kurlovich, D.; Lubnina, N.V.; Nilsson, M.; Orlyuk, M.I.; Pashkevich, I.K.; Shumlyanskyy, L.V.; Starostenko, V.I. Late Palaeoproterozoic mafic dyking in the Ukrainian Shield (Volgo-Sarmatia) caused by rotations during the assembly of supercontinent Columbia. *Lithos* **2013**, *174*, 196–216. [[CrossRef](#)]
69. Shumlyanskyy, L.; Ernst, R.E.; Albekov, A.; Söderlund, U.; Wilde, S.A.; Bekker, A. The early Statherian (ca. 1800–1750 Ma) Prutivka-Novogol large igneous province of Sarmatia: Geochronology and implication for the Nuna/Columbia supercontinent reconstruction. *Precam. Res.* **2021**, *358*, 106185. [[CrossRef](#)]
70. Shumlyanskyy, L.; Hawkesworth, C.; Billström, K.; Bogdanova, S.; Mytrokhyn, O.; Romer, R.; Dhuime, B.; Claesson, S.; Ernst, R.; Whitehouse, M.; et al. The origin of the Palaeoproterozoic AMCG complexes in the Ukrainian Shield: New U-Pb ages and Hf isotopes in zircon. *Precam. Res.* **2017**, *292*, 216–239. [[CrossRef](#)]
71. Shumlyanskyy, L.; Franz, G.; Glynn, S.; Mytrokhyn, O.; Voznyak, D.; Bilan, O. Geochronology of granites of the western Korosten AMCG complex (Ukrainian Shield): Implications for the emplacement history and origin of miarolitic pegmatites. *Eur. J. Mineral.* **2021**, *33*, 703–716. [[CrossRef](#)]
72. Shumlyanskyy, L.; Billström, K.; Hawkesworth, C.; Elming, S.-Å. U-Pb age and Hf isotope compositions of zircons from the north-western region of the Ukrainian shield: Mantle melting in response to post-collision extension. *Terra Nova* **2012**, *24*, 373–379. [[CrossRef](#)]
73. Claesson, S.; Bibikova, E.; Shumlyanskyy, L.; Dhuime, B.; Hawkesworth, C. The oldest crust in the Ukrainian Shield—Eoarchean U-Pb ages and Hf-Nd constraints from enderbites and metasediments. In *Continent Formation through Time*; Van Kranendonk, N.M.W., Parman, S., Shirey, S., Clift, P.D., Eds.; The Geological Society of London: London, UK, 2015; Volume 389, pp. 227–259. [[CrossRef](#)]
74. Claesson, S.; Bibikova, E.V.; Shumlyanskyy, L.; Whitehouse, M.J.; Billström, K. Can oxygen isotopes in magmatic zircon be modified by metamorphism? A case study from the Eoarchean Dniester-Bug Series, Ukrainian Shield. *Precam. Res.* **2016**, *273*, 1–11. [[CrossRef](#)]
75. Stepanyuk, L.M.; Bibikova, E.V.; Claesson, S.; Skobelev, V.M. Sm-Nd isotope systematics of the Precambrian rocks of the western part of the Ukrainian Shield. *Mineral. J. (Ukr.)* **1998**, *20*, 72–79. (In Russian)
76. Shumlyanskyy, L.V.; Stepanyuk, L.M.; Claesson, S.; Rudenko, K.V.; Bekker, A.Y. The U-Pb zircon and monazite geochronology of granitoids of the Zhytomyr and Sheremetiv complexes, the Northwestern region of the Ukrainian Shield. *Mineral. J. (Ukr.)* **2018**, *40*, 63–85. (In Ukrainian) [[CrossRef](#)]
77. Markwick, A.J.W.; Downes, H.; Veretennikov, N. The lower crust of SE Belarus: Petrological, geophysical and geochemical constraints from xenoliths. *Tectonophysics* **2001**, *339*, 215–235. [[CrossRef](#)]
78. Ponomarenko, A.N.; Lesnaya, I.M.; Zyuyltsle, O.V.; Gatsenko, V.A.; Dovbush, T.I.; Kanunikova, L.I.; Shumlyanskyy, L.V. Neoproterozoic of the Ros-Tikych Domain of the Ukrainian Shield. *Geochem. Ore Form.* **2010**, *28*, 11–16. (In Russian)
79. Mints, M.V.; Belousova, E.A.; Konilov, A.N.; Natapov, L.M.; Shchipansky, A.A.; Griffin, W.L.; O'Reilly, S.Y.; Dokukina, K.A.; Kaulina, T.V. Mesoarchean subduction processes: 2.87 Ga eclogites from the Kola Peninsula, Russia. *Geology* **2010**, *38*, 739–742. [[CrossRef](#)]
80. Bogdanova, S.; Gorbatshev, R.; Skridlaite, G.; Soesoo, A.; Taran, L.; Kurlovich, D. Trans-Baltic Palaeoproterozoic correlations towards reconstruction of supercontinent Columbia/Nuna. *Precam. Res.* **2015**, *259*, 5–33. [[CrossRef](#)]
81. Mężyk, M.; Malinowski, M.; Mazur, S. Structure of a diffuse suture between Fennoscandia and Sarmatia in SE Poland based on interpretation of regional reflection seismic profiles supported by unsupervised clustering. *Precam. Res.* **2021**, *358*, 106176. [[CrossRef](#)]